ACS APPLIED MATERIALS & INTERFACES

Research Article

www.acsami.org

Bioinspired Photoelectric Conversion System Based on Carbon-Quantum-Dot-Doped Dye–Semiconductor Complex

Zheng Ma,[†] Yong-Lai Zhang,[‡,§] Lei Wang,[‡] Hai Ming,[†] Haitao Li,[†] Xing Zhang,[†] Fang Wang,[†] Yang Liu,*[,†] Zhenhui Kang,*[,†] and Shuit-Tong Lee*[,†]

[†]Institute of Functional Nano and Soft Materials (FUNSOM) & Jiangsu Key Laboratory for Carbon Based Functional Materials and Devices, Soochow University, Suzhou, 215123, China

[‡]State Key Laboratory on Integrated Optoelectronics, College of Electronic Science and Engineering, Jilin University, 2699 Qianjin Street, Changchun, 130012, China

[§]Center of Super-Diamond and Advanced Films (COSDAF), Department of Physics and Materials Science, City University of Hong Kong, Hong Kong, China

S *Supporting Information*

ABSTRACT: Compared to nature's photoelectric conversion processes, artificial devices are still far inferior in efficiency and stability. Inspired by light absorption and resonance energy transfer processes of chlorophyll, we developed a highly efficient photoelectric conversion system by introducing Carbon quantum dots (CQDs) as an electron transfer intermediary. Compared with conventional dye-sensitized semiconductor systems, the present CQD-doped system showed significantly higher photoelectric conversion efficiency, as much as 7 times that without CQDs. The CQD-doped dye/semiconductor system may provide a powerful approach to the development of highly efficient photoelectric devices.

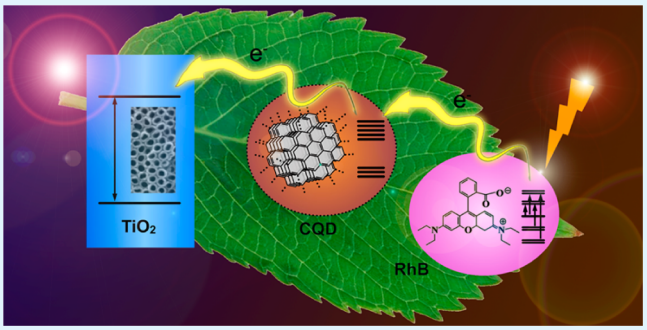

KEYWORDS: *carbon quantum dots, enhanced UV–vis light absorbance, photoelectric conversion, energy transfer, dye–semiconductor complex, power conversion efficiency*

INTRODUCTION

Obtaining energy from sunlight is undoubtedly an effective and attractive solution to the energy-related problems.[1−4] Photoelectric conversion systems based on dye–semiconductor complexes have attracted intense attention because of their diversity and potential for low-cost conversion of photovoltaic energy.[5−11] In this system, to improve the power-conversion efficiency (PCE), a main one among which is charge recombination.[12,13] It occurs at the interface between the porous electrode (most commonly made of TiO_2) and the dye, where photogenerated electrons in the porous electrode tend to recombine with either the oxidized dye or the electrolyte, thereby reducing the photogenerated current, open-circuit voltage, and PCE.[14] One effective approach for mitigating charge recombination is by applying at the electrode/dye interface a insulating energy barrier, such as Al_2O_3[15,16] and Nb_2O_5,[17,18] with improvements in PCE of up to about 35%. However, the application of these charge-recombination barriers have so far relied on the sol–gel process[19,20] and/or atomic layer deposition,[21−25] which require a high temperature treatment (atomic layer deposition may work at relative low temperature), costly equipments, and complex control process.

Green plants in nature possess sophisticated systems for extremely high-efficiency sunlight utilization in narrow spectral range based on the red-peak absorption of chlorophyll (at about 680 nm, 700 nm etc.).[26,27] In those systems, the function of the vast majority of chlorophyll (up to several hundred molecules per photosystem) is to absorb light and transfer that light energy by resonance energy transfer to a specific chlorophyll pair in the reaction center of the photosystems, and then about 97% absorbed light was utilized at reaction center by this manner.[28−31] This process inspires us to insert an additional electron/energy transfer intermediary, instead of the insulating energy barrier, into a dye-semiconductor complex for the design of a highly efficient photoelectric conversion system.

Carbon quantum dots (CQDs) possess fragmented graphitic structure and abundent functional groups on the surface, similar to pigments and polycyclic aromatic hydrocarbons.[32] Such a unique structure gives rise to both up-/down-converted photoluminescence (PL) property and photoinduced electron transfer ability of CQDs.[32,33] In mimicking natural photosystems, CQDs are used as a preferred electron/energy transfer bridge in a dye-semiconductor complex for efficiency enhancement. Here, we report a bioinspired fabrication of dye-

Received: March 14, 2013
Accepted: May 13, 2013
Published: May 13, 2013

semiconductor photoelectric conversion system by incorporating CQDs as an electron/energy transfer intermediary. The addition of CQDs leads to significantly enhanced UV−vis absorbance of RhB. The photocurrent density of the RhB/TiO_2 nanotubes (TiO_2NTs) system doped with CQDs increased to 10 times as high as that without CQDs doping. The remarkable photoinduced electron gain and electron-donating properties make CQDs a promising intermediary for the precise control of photogenerated electron transfer, leading to significant improvement in PCE. The finding holds great promise for the fabrication of high-efficiency photovoltaic devices and light energy conversion systems.

RESULTS AND DISCUSSION

In our experiments, CQDs with sizes of <10 nm or >10 nm are doped into RhB/TiO_2 complex (see the Supporting Information, Figure S1). The as-prepared CQDs possess both water dissolubility and clear graphitic structure owing to the unique preparation route[34] (see the Supporting Information). The presence of these oxygen functional groups (Infrared spectrum of CQDs see Figure S2a in the Supporting Information) imparts water dissolubility to the CQDs. The Raman spectrum of CQDs shows two prominent peaks at 1350 and 1600 cm^{-1}, which are attributed to D and G band, respectively. The D/G intensity ratio (ID/IG) of 1.22, indicates the presence of abundant oxygen defects such as C−O, C═O, O−C═O (see Figure S2b in the Supporting Information).[32,34] The XPS C1s spectrum of CQDs (see Figure S2c in the Supporting Information) also indicates that there are many oxygen groups in CQDs.

Interestingly, the addition of the CQDs into Rhodamine B (RhB) aqueous solution would lead to a significant enhancement of UV−vis absorbance. Figure 1 shows that pure RhB

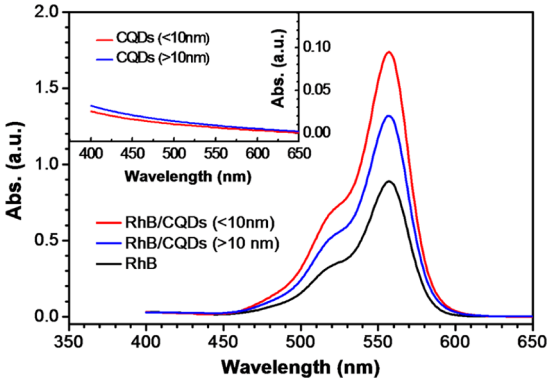

Figure 1. UV−vis absorption spectra of pure RhB and RhB blended with CQDs of different size distribution. The inset shows UV−vis absorption spectra of CQDs of different size distribution.

solution has UV−vis absorbance in the range of 450−600 nm (black curve). Notably, when dye was dissolved in the CQDs solution, an attractive hyperchromic effect appears. The UV−vis absorption of pure RhB solution peaked at 563 nm with an absorbance of about 0.88 (black curve). When RhB was dissolved in CQDs solution with particle size <10 nm and >10 nm, respectively, the absorbance increased to 1.97 times (red curve) and 1.51 times (blue curve) of that for the pure RhB aqueous solution. To exclude the absorption of CQDs in the present RhB/CQDs complex system, the UV−vis absorption spectra of CQDs of two different sizes were also collected for comparison. As shown in the inset of Figure 1, in contrast to the RhB/CQDs complex system, the CQDs only solution shows very weak absorbance of <0.01 at 563 nm, indicating the synergistic hyperchromic effect between RhB and CQDs. Besides, the size of CQDs also shows a significant effect on the absorbance, with smaller CQDs (<10 nm) giving higher enhancement of UV−vis absorption. Here, the absorbance enhancement should be attributed to the electron-donating/-accepting properties and the unique electroconductivity of CQDs, as well as the interaction between CQDs and dye molecules (decreases molecule coplanarity and disturbs the conjugation).[3,32,35,36]

In general, enhanced absorption of RhB/CQDs complex would contribute to light harvesting, consequently promoting the photoelectric conversion efficiency of the dye−semiconductor complex system. To evaluate the energy and/or electron transfer process and the photoelectrochemical properties in the CQDs/RhB/TiO_2 complex, we carried out a series of photoelectrochemical experiments in a two-electrode cell system with platinum wire as the counter electrode. The TiO_2NTs fabricated by anodization of Ti foils was used as the working electrode. As the SEM images (see Figure S3a, b in the Supporting Information) show, the TiO_2NTs are 60−80 nm in diameter and ∼2 μm in length. Moreover, all peaks in the XRD pattern of TiO_2NTs shown in Figure S3c in the Supporting Information can be indexed to Ti metal phase and TiO_2 anatase phase, respectively. TiO_2NTs doped with RhB and RhB/CQDs hybrids were measured for comparison. The RhB/CQDs/TiO_2 electrodes were prepared by using a simple wet impregnation method (see the Supporting Information). Figure 2 shows the

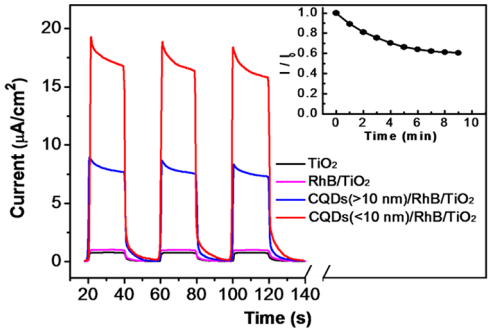

Figure 2. Photocurrent density versus time curves of TiO_2 nanotubes, RhB/TiO_2, and RhB/TiO_2 doped with CQDs of different size. The results were measured in 0.1 M Na_2SO_4 solution under simulated sunlight irradiation (33 mW cm^{-2}). The inset shows the time dependence of photocurrent density of CQDs (<10 nm) /RhB/TiO_2, where I and I_0 denote the instantaneous and starting density, respectively.

photoelectrical responses (instantaneous change in current upon illumination) of different anodes (TiO_2NTs, RhB/TiO_2NTs, and CQDs/RhB/TiO_2NTs) under intermittent illumination. The short-circuit photocurrent density of TiO_2NTs was 0.76 μA cm^{-2} (black curve), while that of RhB/TiO_2NTs slightly increased to 1.01 μA cm^{-2} (red curve), indicating the contribution of dye molecules. Remarkably, when CQDs were doped into the RhB/TiO_2 complex, the photocurrent density sharply increased 9.5 times for CQDs of >10 nm and 21.1 times for CQDs of <10 nm. The observation that CQDs with particle size below 10 nm show the highest enhancement is consistent with the results of UV−vis

dx.doi.org/10.1021/am400930h | ACS Appl. Mater. Interfaces 2013, 5, 5080−5084

absorption. The inset of Figure 2 shows the dependence of photocurrent density of the CQDs (<10 nm)/RhB/TiO_2NTs on decay time. After 10 min of sunlight irradiation, the photocurrent density decreased to an equilibrium value of ~60.6%. The short-circuit photocurrent density of CQDs/TiO_2NTs has also been measured. Compared to TiO_2NTs, the photocurrent density of CQDs/TiO_2NTs slightly increased to 0.93 μA cm^{-2} (see Figure S3d in the Supporting Information), suggesting the enhanced current of the complex system is due to the synergistic effect of the dye molecule and CQDs.

Because CQDs play the instrumental role in achieving high photocurrent density, we therefore investigated the electron-accepting and -donoring properties of CQDs by evaluating the luminescence decays of CQDs in the presence of different quenchers (2,4-dinitrotoluene, electron acceptors; N,N-diethylaniline, electron donors; see Figure S4 in the Supporting Information).[37] The results show that CQDs are both electron donors and acceptors, leading to efficient luminescence quenching by known electron donors and acceptors under visible-light irradiation. The photomediated electron-accepting and electron-donating properties make the CQDs an excellent electron transfer intermediary for both effective charge separation and suppression of charge recombination.

To obtain further insight into the mechanism of the synergistic effect of RhB and CQDs, we examined the PL quenching dynamics of RhB blended with CQDs, and compared the femtosecond transient absorption spectroscopy of RhB/TiO_2 systems with and without CQDs (Figure 3a, b).

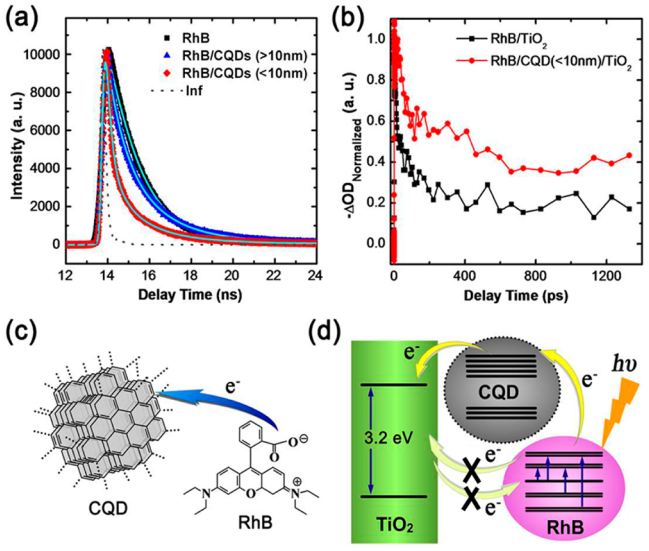

Figure 3. (a) Photoluminescence quenching of RhB and RhB/CQDs complex measured by time-correlated single photon counting (TCSPC) technique. (b) Ground-state bleaching recovery of RhB molecules in RhB/TiO_2 and RhB/CQD/TiO_2 complex systems extracted from femtosecond transient absorption (TA) spectroscopy. (c) Scheme of electron transfer from RhB to CQDs. (d) CQDs serve as an electron transfer intermediary for bridging the photogenerated electrons and suppressing their recombination.

When RhB was dissolved in CQDs solution, the PL of RhB is effectively quenched, as shown in Figure S5 in the Supporting Information. The corresponding PL lifetime of RhB in CQDs solution with particle sizes >10 nm and <10 nm decreased to 1.35 ns (blue triangle) and 0.52 ns (red diamond), respectively, from 1.53 ns for pure aqueous RhB solution. It demonstrates the dynamic PL quenching in the RhB/CQDs system, which is attributable to electron transfer from RhB to CQDs, as shown in Figure 3c.

For the RhB/TiO_2 and RhB/CQDs(<10 nm)/TiO_2 complex anode systems, the role of CQDs is further demonstrated by the femtosecond transient absorption (TA) spectroscopy (see Figure S6 in the Supporting Information). Compared with the ground state bleaching recovery of RhB molecules in the RhB/TiO_2 system (Figure 3b), the RhB/CQD/TiO_2 complex system shows significantly more unrecovered RhB molecules in the long time scale (~1 ns). This indicates the back electron transfer from TiO_2 to RhB has been considerably inhibited, significantly decreasing the loss of photoinduced carriers. As shown in Figure S7 in the Supporting Information, the kinetics in the long delay time is normalized, whereas the magnitude of absorptive signal at around 500 nm is about two times larger in CQD-treated RhB/TiO_2 films with respect to untreated films. This result implies that the back electron transfer from TiO_2 to RhB is suppressed in the first 20 ps. This extra change is consistent with the dynamics of bleaching signal shown in Figure 3b. So the transient absorption data supports our proposed mechanism well. These results show that CQDs in the dye/semiconductor systems, as shown in Figure 3d, serve as an electron transfer intermediary that can bridge the photogenerated electrons and efficiently suppress their recombination.

To further assess the photoelectric conversion efficiency, a CQD-bridged and RhB-sensitized TiO_2-based solar cell system has been fabricated (experimental details in the Supporting Information). In the following experiments, we also investigated the synergistic effect of CQDs and RhB in the CQD-bridged dye-sensitized solar cell (C-DSC) system. In our work, the obtained power conversion efficiency (PCE) is 0.147%, which is seven times larger than that without CQD bridging. The significantly enhanced PCE could be mainly attributed to the large increase in short circuit current density (J_{sc}), despite a slight decrease in open circuit voltage (V_{oc}) and fill factor, as shown in Figure 4. Our experiments further showed that the

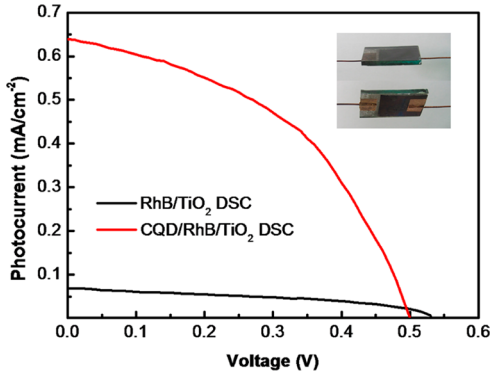

Figure 4. $J-V$ characteristics of RhB-sensitized TiO_2NTs solar cells doped with and without CQDs under AM1.5 G (100 mW cm^{-2}) illumination. The inset is the photo image of the C-DSC.

PCE of the present C-DSCs system decayed to and stabilized at ~0.103% after 60 min continuous illumination, which is similar to the photocurrent density decrease behavior of the CQDs/RhB/TiO_2NTs system. Although the device performance needs much further improvement, the present system has the benefit that it can be optimized by introduction of different nanostructures (nanowires, -rods, -tubes, and their arrays) of

dx.doi.org/10.1021/am400930h | ACS Appl. Mater. Interfaces 2013, 5, 5080−5084

semiconductors (ZnO, NiO, SnO, WO_3, etc.).[38] Further, CQDs of proper size and surface modification, as well as doping with nonmetals, such as S, N, P, and B, may also improve device performance.[39−42] Given the diversity and versatility of structural design of the present system, the combination of CQDs and dye/semiconductor system should provide a promising approach toward the design of intelligent and highly efficient photoelectric devices.

CONCLUSION

In conclusion, inspired by natural photosystems, we develop a CQDs-bridged dye/semiconductor complex system for the fabrication of high-efficiency photoelectric conversion systems. Experimental results show that the presence of CQDs not only can enhance the UV−vis absorbance of RhB solutions, but also effectively suppress the recombination of photogenerated electrons, thereby leading to significantly enhanced photoelectric conversion efficiency. Investigation of PL quenching dynamics of RhB/CQDs mixture and transient absorption of RhB/CQDs/TiO_2 complex showed that CQDs could act as a one-way electron transfer intermediary for effective bridging of RhB molecules and TiO_2 substrate. Doping of CQDs into the dye/semiconductor complex significantly improved the photoelectric conversion efficiency of the complex by ∼7 times. The findings would be of great importance to the development of high-efficiency photoelectronic devices.

ASSOCIATED CONTENT

Supporting Information

Experimental section, TEM image and size distribution of CQDs (>10 nm and <10 nm), Raman and FTIR spectrum of CQDs < 10 nm, photocurrent density versus time curves, luminscence decays results,and TA results. This material is available free of charge via the Internet at http://pubs.acs.org.

AUTHOR INFORMATION

Corresponding Author

*E-mail: yangl@suda.edu.cn (Y.L.); zhkang@suda.edu.cn (Z.K.); apannale@suda.edu.cn (S.-T.L.).

Notes

The authors declare no competing financial interest.

ACKNOWLEDGMENTS

This work is supported by the National Basic Research Program of China (973 Program) (2012CB825800, 2013CB932702), the National Natural Science Foundation of China (51132006, 61008014, 21073127, 21071104), the Specialized Research Fund for the Doctoral Program of Higher Education (20123201110018), a Suzhou Planning Project of Science and Technology (ZXG2012028), a Foundation for the Author of National Excellent Doctoral Dissertation of China (200929), and a project funded by the Priority Academic Program Development of Jiangsu Higher Education Institutions. We also acknowledge the Hong Kong Scholar Program (XJ2011014).

REFERENCES

(1) Graetzel, M. *Acc. Chem. Res.* **2009**, *42*, 1788−1798.
(2) Kubacka, A.; Fernandez-Garcia, M.; Colon, G. *Chem. Rev.* **2012**, *112*, 1555−1614.
(3) Li, H. T.; Kang, Z. H.; Liu, Y.; Lee, S. T. *J. Mater. Chem.* **2012**, *22*, 24230−24253.
(4) Wang, P.; Zakeeruddin, S. M.; Moser, J. E.; Nazeeruddin, M. K.; Sekiguchi, T.; Gratzel, M. *Nat. Mater.* **2003**, *2*, 402−407.
(5) Bach, U.; Lupo, D.; Comte, P.; Moser, J. E.; Weissortel, F.; Salbeck, J.; Spreitzer, H.; Gratzel, M. *Nature* **1998**, *395*, 583−585.
(6) Yao, Q. H.; Meng, F. S.; Li, F. Y.; Tian, H.; Huang, C. H. *J. Mater. Chem.* **2003**, *13*, 1048−1053.
(7) Kiema, G. K.; Colgan, M. J.; Brett, M. J. *Sol. Energy Mater. Sol. Cells* **2005**, *85*, 321−331.
(8) Ardo, S.; Sun, Y. L.; Staniszewski, A.; Castellano, F. N.; Meyer, G. J. *J. Am. Chem. Soc.* **2010**, *132*, 6696−6709.
(9) Jennings, J. R.; Ghicov, A.; Peter, L. M.; Schmuki, P.; Walker, A. B. *J. Am. Chem. Soc.* **2008**, *130*, 13364−13372.
(10) Concepcion, J. J.; Jurss, J. W.; Brennaman, M. K.; Hoertz, P. G.; Patrocinio, A. O. T.; Murakami Iha, N. Y.; Templeton, J. L.; Meyer, T. J. *Acc. Chem. Res.* **2009**, *42*, 1954−1965.
(11) Ito, S.; Zakeeruddin, S. M.; Comte, P.; Liska, P.; Kuang, D.; Graetzel, M. *Nat. Photonics* **2008**, *2*, 693−698.
(12) Durrant, J. R.; Haque, S. A.; Palomares, E. *Coordin. Chem. Rev.* **2004**, *248*, 1247−1257.
(13) Lin, C.; Tsai, F. Y.; Lee, M. H.; Lee, C. H.; Tien, T. C.; Wang, L. P.; Tsai, S. Y. *J. Mater. Chem.* **2009**, *19*, 2999−3003.
(14) Hardin, B. E.; Snaith, H. J.; McGehee, M. D. *Nat. Photonics* **2012**, *6*, 162−169.
(15) Palomares, E.; Clifford, J. N.; Haque, S. A.; Lutz, T.; Durrant, J. R. *Chem. Commun.* **2002**, 1464−1465.
(16) Palomares, E.; Clifford, J. N.; Haque, S. A.; Lutz, T.; Durrant, J. R. *J. Am. Chem. Soc.* **2003**, *125*, 475−482.
(17) Zaban, A.; Chen, S. G.; Chappel, S.; Gregg, B. A. *Chem. Commun.* **2000**, 2231−2232.
(18) Xia, J.; Masaki, N.; Jiang, K.; Yanagida, S. *Chem. Commun.* **2007**, 138−140.
(19) Ito, S.; Ha, N. L. C.; Rothenberger, G.; Liska, P.; Comte, P.; Zakeeruddin, S. M.; Péchy, P.; Nazeeruddin, M. K.; Grätzel, M. *Chem. Commun.* **2006**, 4004−4006.
(20) Liu, X.; Luo, Y.; Li, H.; Fan, Y.; Yu, Z.; Lin, Y.; Chen, L.; Meng, Q. *Chem. Commun.* **2007**, 2847−2849.
(21) Roh, S. J.; Mane, R. S.; Min, S. K.; Lee, W. J.; Lokhande, C. D.; Han, S. H. *Appl. Phys. Lett.* **2006**, *89*, 253512:1−3.
(22) Hod, I.; Shalom, M.; Tachan, Z.; Ruhle, S.; Zaban, A. *J. Phy. Chem. C* **2010**, *114*, 10015−10018.
(23) Chandiran, A. K.; Tetreault, N.; Humphry-Baker, R.; Kessler, F.; Baranoff, E.; Yi, C. Y.; Nazeeruddin, M. K.; Gratzel, M. *Nano Lett.* **2012**, *12*, 3941−3947.
(24) Prasittichai, C.; Hupp, J. T. *J. Phys. Chem. Lett.* **2010**, *1*, 1611−1615.
(25) Katz, M. J.; Vermeer, M. J. D.; Farha, O. K.; Pellin, M. J.; Hupp, J. T. *Langmuir* **2013**, *29*, 806−814.
(26) Hagfeldt, A.; Boschloo, G.; Sun, L. C.; Kloo, L.; Pettersson, H. *Chem. Rev.* **2010**, *110*, 6595−6663.
(27) Wasielewski, M. R. *Chem. Rev.* **1992**, *92*, 435−461.
(28) Wang, X. F.; Xiang, J. F.; Wang, P.; Koyama, Y.; Yanagida, S.; Wada, Y.; Hamada, K.; Sasaki, S.; Tamiaki, H. *Chem. Phys. Lett.* **2005**, *408*, 409−414.
(29) Wang, X. F.; Kitao, O.; Zhou, H.; Tamiaki, H.; Sasaki, S. i. *Chem. Commun.* **2009**, 1523−1525.
(30) Wang, X. F.; Koyama, Y.; Kitao, O.; Wada, Y.; Sasaki, S. i.; Tamiaki, H.; Zhou, H. *Biosens. Bioelectron.* **2010**, *25*, 1970−1976.
(31) Wang, X. F.; Tamiaki, H.; Wang, L.; Tamai, N.; Kitao, O.; Zhou, H.; Sasaki, S. i. *Langmuir* **2010**, *26*, 6320−6327.
(32) Li, H. T.; He, X. D.; Kang, Z. H.; Huang, H.; Liu, Y.; Liu, J. L.; Lian, S. Y.; Tsang, C. H. A.; Yang, X. B.; Lee, S.-T. *Angew. Chem., Int. Ed.* **2010**, *49*, 4430−4434.
(33) Li, H. T.; He, X. D.; Liu, Y.; Huang, H.; Lian, S. Y.; Lee, S. T.; Kang, Z. H. *Carbon* **2011**, *49*, 605−609.
(34) Ming, H.; Ma, Z.; Liu, Y.; Pan, K. M.; Yu, H.; Wang, F.; Kang, Z. H. *Dalton* **2012**, *41*, 9526−9531.
(35) Zawadiak, J.; Mrzyczek, M. *Spectrochim. Acta A* **2012**, *96*, 815−819.

(36) Hua, J.; Wang, Z. G.; Xu, L.; Wang, X.; Zhao, J.; Li, F. F. *Mater. Chem. Phys.* **2013**, *137*, 694−698.
(37) Wang, X.; Cao, L.; Lu, F. S.; Meziani, M. J.; Li, H. T.; Qi, G.; Zhou, B.; Harruff, B. A.; Kermarrec, F.; Sun, Y. P. *Chem. Commun.* **2009**, 3774−3776.
(38) Satvasheel, P.; Torben, D.; Michelle, T. M.; Dongchuan, F.; Noel, W. D.; Gunther, G.; Martin, W.; Amaresh, M.; Peter, B.; Leone, S.; Udo, B. *Angew. Chem., Int. Ed.* **2013**, *52*, 602−605.
(39) Wohlgemuth, S. A.; White, R. J.; Willinger, M. G.; Titirici, M. M.; Antonietti, M. *Green Chem.* **2012**, *14*, 1515−1523.
(40) Fellinger, T. P.; Hasche, F.; Strasser, P.; Antonietti, M. *J. Am. Chem. Soc.* **2012**, *134*, 4072−4075.
(41) Liang, J.; Jiao, Y.; Jaroniec, M.; Qiao, S. Z. *Angew. Chem., Int. Ed.* **2012**, *51*, 11496−11500.
(42) Yang, D. S.; Bhattacharjya, D.; Inamdar, S.; Park, J.; Yu, J. S. *J. Am. Chem. Soc.* **2012**, *134*, 16127−16130.